Desalination and Water Treatment
www.deswater.com

doi: 10.5004/dwt.2018.23067

129 (2018) 101–115
October

Effects of ultrasonic irradiation on organic matter of *Microcystis aeruginosa* cells

Gongduan Fan[a,*,†], Huiping Peng[a,†], Xiaomei Zheng[a], Jing Luo[b], Wei Chen[a]

[a]*College of Civil Engineering, Fuzhou University, 350116 Fujian, China; email: fgdfz@fzu.edu.cn (G. Fan), Tel. +0086 591 22865361; Fax: +0086 591 22865355; emails: n160527036@fzu.edu.cn (H. Peng), n160520053@fzu.edu.cn (X. Zheng), n150520048@fzu.edu.cn (W. Chen)*
[b]*Fujian Minke Environmental Technology Development Co., Ltd, Fuzhou, 350002 Fujian, China; email: 727919985@qq.com*

Received 24 February 2018; Accepted 28 August 2018

ABSTRACT

Harmful algal bloom stimulated by eutrophication has gained increasing attention worldwide. This phenomenon deteriorates water quality and destroys the local ecological equilibrium, and thus must be addressed. Ultrasound can effectively inhibit the growth of bloom algae, but its effect on the organic matter of *Microcystis aeruginosa* cells remains unknown. Moreover, the mechanism of ultrasonic irradiation is unclear. This study investigated algal biomass, zeta potential, organic matter, and protein after treatment with different ultrasonic frequencies and power densities to optimize ultrasonic parameters and reveal the mechanism of the effect of ultrasonic irradiation on algae. Results showed that low-frequency ultrasonic irradiation effectively inhibited blue algae growth. The zeta potential, ribulose-1,5-bisphosphate carboxylase/oxygenase (RuBisCO) protein gray value, and phycobiliprotein level decreased, whereas the fluorescence peak of fulvic acid and dead cells increased. The damage to the RuBisCO protein in algae treated by ultrasonic frequency of 40 kHz was more severe than that in algae treated by the frequency of 20 and 100 kHz under the power density of 0.0628 W/mL. The high ultrasonic density caused severe damage to the RuBisCO protein and photosynthesis. Under a specific ultrasonic frequency, higher power density leads to more obvious inhibition on algae cells. Thus, the growth of *M. aeruginosa* can be controlled under the optimal ultrasonic frequency and power density of 40 kHz and 0.0628 W/mL, respectively.

Keywords: Ultrasound; *Microcystis aeruginosa*; Organic matter; Inhibition; Phycobiliprotein; Photosynthetic protein

1. Introduction

The incidence of cyanobacterial blooms stimulated by water eutrophication has increased worldwide. Cyanobacterial blooms cause water quality degradation, aquatic ecosystem imbalance, bad odor, and microcystin release [1–3], which lead to indiscriminate killing of fishes and invertebrates in water, various health problems to humans, and high cost of water treatment [4,5]. Therefore, control and prevention of cyanobacterial bloom have become a pressing global issue [6]. At present, engineering methods, chemical processes, biological control, and modified clay technology are the four main measures used to control cyanobacterial blooms; examples of them include blocking the sunlight, adding algal-inhibiting agent or algicide, and introducing algae eaters [7,8]. However, these processes exhibit disadvantages, such as high cost, complex operation, and secondary pollution, which limit their application [9].

Scholars have focused on controlling algal growth by ultrasonic irradiation. This method can remove algal toxins while being used to control cyanobacterial blooms [10]. Ultrasonic irradiation can damage the photosynthetic system of algae by continuously decreasing the chlorophyll a content [10]. A previous research reported that high-frequency ultrasonic irradiation led to severe

* Corresponding author.

† These authors contributed equally to this work and should be considered as co-first authors.

damages to *Melosira granulate* [11]. Klemenčic et al. [12] proposed the use of ultrasonic irradiation to effectively sink floating algae. Numerous studies have investigated on inhibiting algal growth by ultrasonic irradiation [13,14], but the effect of such method on the organic matter of algal cells has not been thoroughly studied.

Algae contain organic matter, such as phycoerythrin (PE), phycocyanin (PC), allophycocyanin (APC), D1 protein, ribulose-1,5-bisphosphate carboxylase/oxygenase (RuBisCO) protein, chlorophyll a, tryptophan, and tyrosine. Extracellular organic matter (EOM) is formed by the metabolism of algal cells in water, and intracellular organic matter (IOM) is formed by the decomposition of algal cells [15]. Organic matter is released into the water during the apoptosis of algal cells. Analysis of three-dimensional excitation–emission matrix (EEM) indicated that organic matter of algae consists of protein and humus [16]. Liu et al. [17] determined the three-dimensional EEM fluorescence spectra of EOM and IOM under ultrasonic irradiation for different durations. The concentrations of protein, plastic organic matter, and dissolved organic nitrogen increased with time. However, limited information is available regarding the effect of different ultrasonic parameters on organic matter inside algae [17]. Organic matter synthesis is related to light energy. The use of ultrasound to treat *Microcystis aeruginosa* cells can damage the photosynthetic system and cause phycobiliprotein content degradation [18] and phycobilisome damage [19]. Thus, algal cells cannot synthesize organic matter with light energy. Few researchers have studied the effect of different ultrasound parameters on inhibiting algal growth by monitoring changes in organic matter. In this work, the optimum combination of ultrasonic parameters for inhibiting the growth of cyanobacterial blooms was determined based on changes in the total organic matter content and composition in algae cells. The effects of different ultrasonic parameters on the control of algae biomass were also compared. Results provide a theoretical basis for large-scale application of ultrasonic technology to inhibit algal growth in water.

2. Materials and methods

2.1. Algae culture and ultrasonic processing

M. aeruginosa cells (FACHB-905, obtained from the Dian Lake in China) was purchased from the Freshwater Algae Culture Collection at the Institute of Hydrobiology in Wuhan, China. The cells were cultured in BG-11 growth medium at 30°C ± 1 °C under light–dark cycle of 14 h:10 h with cold incandescent light as source and illumination intensity of 2,000 lx [20]. The initial pH of the medium is close to 7.0 [21].

Algal cell suspension was treated with 20, 40, and 100 kHz of ultrasound. The untreated samples were used as control. The fluid volume of algae in the experimental groups treated with ultrasonic irradiation for 5 min was 100 mL per bottle, and the culture conditions were the same as those used in the control groups. The suspension of algal cells was subjected to ultrasound at different frequencies (20, 40, and 100 kHz) and a fixed power density of 0.013 W/mL; and different power densities (0.0126, 0.0224, and 0.0628 W/mL) and a fixed frequency of 40 kHz. The treated samples were cultured in an incubator for 2, 24, 48, 96, and 144 h and then analyzed.

2.2. Detection of zeta potential

Zeta potential of the samples was measured by a laser particle size analyzer (Zetasizer Nano ZS, Malvern, UK), which can detect the charges of the algal solution.

2.3. Detection of three-dimensional fluorescence spectrum

2.3.1. Extraction of EOM

EOM of algae was collected using a high-speed refrigerated centrifuge [22]. The algal samples were centrifuged at 5,000 rpm and 4°C for 10 min. The cell-free supernatant was filtered through 0.45 μm membrane, and organic matter in the filtrate represented EOM.

2.3.2. Extraction of IOM

IOM was collected using the method of Tian et al. [23]. Algal samples were centrifuged at 5,000 rpm for 10 min, and the precipitate was washed by deionized (DI) water three times to remove the interference of culture solution on the algae cell surface. The solution was added with DI water (DI water/algae = 15 mL/g) and frozen and thawed twice. The samples were then treated by an ultrasonic cell crusher for 30 min to completely release IOM. The samples were collected after centrifugation at 5,000 rpm for 10 min and filtered through a 0.45-μm glass fiber filter. The cell-free enzyme supernatant was placed in brown bottles at 4°C for further use.

2.3.3. Detection of three-dimensional EEM

Algal EOM and IOM were detected using a fluorescence spectrophotometer (FS5, Edinburgh Instruments, UK) through fluorescence spectrum scanning. Detection was conducted using a 1-cm quartz fluorescence sample cell at room temperature. Laser light illumination was provided by a 150-W xenon lamp. The slits of grating for excitation and emission were of 1.4 nm. The spectra with excitation from 200 to 750 nm at 5 nm increments and emission from 200 to 800 nm at 5 nm increments were scanned.

2.4. Detection of photosynthetic protein

2.4.1. Extraction and determination of total protein

Total protein of *M. aeruginosa* was extracted according to the method of Tao et al. [6]. In brief, 50 mL of the algal suspension was centrifuged at 5,000 rpm and 4°C for 10 min to collect algal cells. The cells were resuspended in phosphate-buffered saline (PBS) solution and centrifuged. The cell-free enzyme supernatant was deposited on ice to prevent protein degradation because of the hot temperature during the addition of the lysis buffer. The sample was mixed with 100 μL of lysis buffer, frozen in liquid nitrogen for 15 s, and unfrozen with an ultrasonic cell crusher; these processes were repeated three times. All samples were centrifuged at 5,000 rpm and 4°C for 10 min, and the suspension represented the total protein of *M. aeruginosa*. Total protein concentration was detected using the bicinchoninic acid (BCA) protein assay kit (Beyotime, China) [6].

2.4.2. Detection of the RuBisCO protein

The RuBisCO protein of *M. aeruginosa* was detected through Western blot analysis according to the method of Six et al. [24]. The sample (90 μL) was mixed with 30 μL of dithiothreitol (DTT) sodium dodecyl sulfate - polyacrylamide gel electrophoresis (SDS-PAGE) loading buffer (4×). The degenerated protein was placed in a metal bath at 99°C and 350 rpm for 5 min. The protein was separated by SDS electrophoresis with 12% of separating gel. The protein was then transferred from the separating gel onto the polyvinylidene fluoride (PVDF) membrane (IPVH00010 0.45 μm, Millipore, USA) that was activated with methanol. The method was called semi-dry method. The PVDF membrane was placed in blocking buffer (SW3015-100 mL, Solarbio, China) and incubated at room temperature for 1 h to maintain the specificity of the primary antibodies. The membrane was then incubated with primary antibody (anti-RbcL; RuBisCO large subunit, forms I and II;AS03037, Agrisera, Sweden) overnight. The PVDF membrane was incubated in secondary antibody (goat anti-rabbit conjugate acid radical peroxidase) after washing in TBST three times (10 min each). The membrane was then washed in TBST three times for 10 min for the first two washes and for 15 min for the last wash. An enhanced chemiluminescence (ECL) chemiluminescence detection kit (E411-04, Vazyme, China) was used to develop and analyze protein bands.

2.5. Detection of phycobiliprotein

In brief, 3 mL of the sample was centrifuged at 5,000 rpm for 10 min to collect algal cells and washed twice in PBS solution. The sample was added with 1.5 mL of the PBS solution, maintained at –20°C for 4 h, and incubated in the dark for 30 min at room temperature to shock the melt. The sample was then subjected to two cycles of freezing and thawing. The homogenate was centrifuged at 5,000 rpm for 10 min. The cell-free supernatant was collected for photometer detection at A_{565}, A_{620}, and A_{650}.

2.6. Algal density and inhibition rate

A blood counting chamber (1 mm × 1 mm × 0.1 mm) was used to count the number of algae cells. The absorbance of normal algal cell suspension was detected by fluorescence, which was also used to plot the standard curves of algae density and absorbance (OD_{560}) and can be found in Fig. S1. The data of the treatment and control groups were calculated by the standard curves.

The inactivation efficiency of *M. aeruginosa* cells treated by ultrasound was measured by inactivation rate (I_r) [25] based on the growth rate of cells. I_r was calculated according to the following equation:

$$I_r(\%) = \frac{v_c - v_T}{v_c} \times 100 = \left(\frac{1 - \ln N_{T_i} - \ln N_{T_0}}{\ln N_{C_i} - \ln N_{C_0}} \right) \times 100 \quad (1)$$

where I_r is the inactivation rate based on the growth rate of cells (%), v_C is the growth rate of control cells, v_T is the growth rate of treatment cells, N_{T_i} is the algal density of treatment groups that had been cultured for time i (h), N_{T_0} is the initial algal density of treatment groups, N_{C_i} is the algal density of control groups that cultured for time i (h), and N_{C_0} is the initial algal density of control groups.

2.7. Data analysis

Data were analyzed using Microsoft Excel, Origin8.0, and IBM SPSS Statistics 18. The protein bands were analyzed using Image Lab 3.0.

3. Results and discussion

3.1. Zeta potential of algal cells

Zeta potential can reflect the stability of algal solution in aqueous solutions. Algal cells were negatively charged [26]. Metabolites produced by metabolic activity in algal cells were adsorbed to cell surface resulting in an increased electronegativity [27]. The algal cells that died or were disrupted by sonication decreased the algal solution stability.

The changes in the zeta potential under ultrasound exposure with different frequencies and a fixed power density of 0.013 W/mL are shown in Fig. 1(a). The zeta potentials of the algal solution after ultrasound treatment at

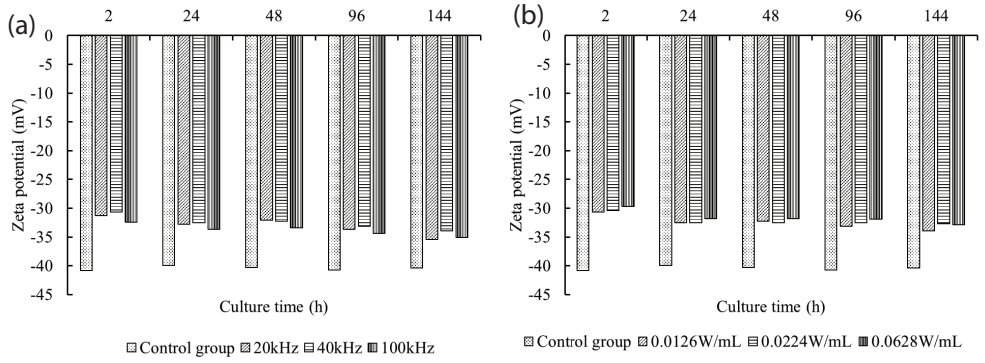

Fig. 1. Zeta potential after ultrasonic irradiation with (a) different frequencies and a fixed power density of 0.013 W/mL, and (b) different power densities and a fixed frequency of 40 kHz.

different ultrasonic frequencies of 20, 40, and 100 kHz were similar. The greater the absolute value of the zeta potential is, the more stable the solution would be. As shown in Fig. 1(a), the zeta potential changed in different degrees under different ultrasonic frequencies, illustrating that the degree of coagulation changed. However, the degree of coagulation with different ultrasonic frequencies showed no significant difference. The increased zeta potential in the control group (40 mV) showed improved stability of the solution because the algal solution contains soluble EOM. Ultrasonic cavitation led to the change in the cell structure under ultrasound, thereby changing the cohesiveness of algal cells. The zeta potential changed from –40.8 to –29.7 mV, electronic conductivity fell from 3.19 to 3.09 mS/cm, and the liquidity increased from –3.196 to –2.394 μm cm/VS after ultrasound treatment (Table 1), which improved the cohesiveness of the solution that was good for the separation of the algae from water.

The changes in the zeta potential of the algal solution after exposure to ultrasound under different power densities with a fixed ultrasonic frequency of 40 kHz are shown in Fig. 1(b). The trends of zeta potential with the power densities of 0.0126, 0.0224, and 0.0668 W/mL were nearly identical. As shown in Fig. 1(b), the greater the power density is, the greater the degree of coagulation would be. The high power density is, therefore, beneficial to the coagulation of algal solution at a fixed frequency.

3.2. The three-dimensional EEM on algae cells

3.2.1. The three-dimensional EEM of total organic matters in algae cells

Algal EOM and IOM contained a lot of polymeric substances, such as proteins, peptides, and amino acids. The protein content of IOM is much higher than that of EOM [28]. Three-dimensional EEM fluorescence spectra can roughly analyze the content of algal organic matter containing proteins and humus.

The changes in the EEM fluorescence spectra under ultrasound exposure with different frequencies and a fixed power density of 0.013 W/mL are shown in Fig. 2. The spectra included three kinds of fluorescence peaks, including Peak A (PC) at E_x/E_m = 620 nm/650 nm [29], Peak B (chlorophyll a) at E_x/E_m = 440 nm/680 nm [30,31], and Peak C (tryptophan and tyrosine) at E_x/E_m = 275 nm/340 nm [32]. As seen in Fig. 2, the peaks A, B, and C of the algal cells continued to rise in the control group within 2–144 h, which explained that the algal cells grew well. After 24 h of treatment, the increase of peaks A, B, and C revealed that the repair mechanism was initiated after ultrasonic treatment. During 48–144 h, the fluorescence spectrum peaks of algal cells began to decrease in the experimental groups. The result showed that the cellular repair mechanism was unable to repair the cells to the original level. When the power density was the same, the damage of algal cells at different ultrasonic frequencies of 20, 40, and 100 kHz was almost the same. The result suggested that low frequency could reduce the damage to algal cells. Thus, the damage degrees of algal cells were not pronounced.

Table 1
Zeta potential of samples before and after the ultrasonic treatment

Sample	Zeta potential (mV)	Electronic conductivity (mS/cm)	Liquidity (μm·cm/VS)
Control group (0 d)	–40.8	3.19	–3.196
40 kHz, 0.013 W/mL (0 d)	–30.5	3.09	–2.394

The changes in EEM under ultrasound exposure with different power densities and a fixed ultrasonic frequency of 40 kHz are shown in Fig. 3. The peaks A, B, and C of the algal cells also continued to rise in the control group within 2–144 h. In 2–144 h, the decrease of peaks A, B, and C revealed that the protein chlorophyll a, tryptophan, and tyrosine were destroyed with the power densities of 0.0224 and 0.0628 W/mL. The greater power density and lower the fluorescence spectrum peak, the more severe the lesion of algal cells. The damage of protein chlorophyll a, tryptophan, and tyrosine could influence the cellular uptake and proliferation [33]. The trend was almost the same as the trend of algal density change.

3.2.2. EOM three-dimensional fluorescence of algae cells

The three-dimensional EEM fluorescence spectra of EOM under ultrasound with different frequencies and a fixed power density of 0.013 W/mL are presented in Fig. S2. The three kinds of fluorescence peaks included in the spectra are Peak A (humic acid type matters) E_x/E_m = (350–440) nm/(430–510) nm, Peak B (soluble metabolites) E_x/E_m = (270–290) nm/(330–350) nm, and Peak C (fulvic acid in the ultraviolet region) E_x/E_m = (260–275) nm/(421–464) nm [34,35]. As seen in Fig. S2, the peaks A, B, and C of the algal cells continued to rise in the control group within 2–144 h illustrating that the algal cells grew well. In 2 h, the decrease of peaks A, B, and C revealed that the cell death and the release of algal cell intracellular products were due to the ultrasonic treatment in the different experimental groups. In 24–144 h, the increase of peaks A and C revealed that increasing amounts of humic and fulvic acid substances were released into the solution after ultrasonic treatment but the discrimination was not obvious.

The change in Peak B was different from those in peaks A and C. The EEM fluorescence spectra exhibited a strong fluorescence characteristic at the fluorescence Peak B. The peak value of fluorescence Peak B significantly decreased after ultrasonic action at different frequencies. We suggested that the fluorescence peak of Peak B decreased due to the ultrasonic treatment. Subsequently, the fluorescence peak of Peak B was elevated. The elevation might be because the cellular repair mechanism was unable to return to the initial level of the fluorescence peak after the ultrasonic treatment. The elevation showed that ultrasound had definite inhibitory effect on the growth of algal cells.

Three-dimensional EEM fluorescence spectra of EOM under ultrasound with different power densities and a fixed frequency of 40 kHz are presented in Fig. S3. The peaks A, B, and C of the algal cells continued to rise in the control group

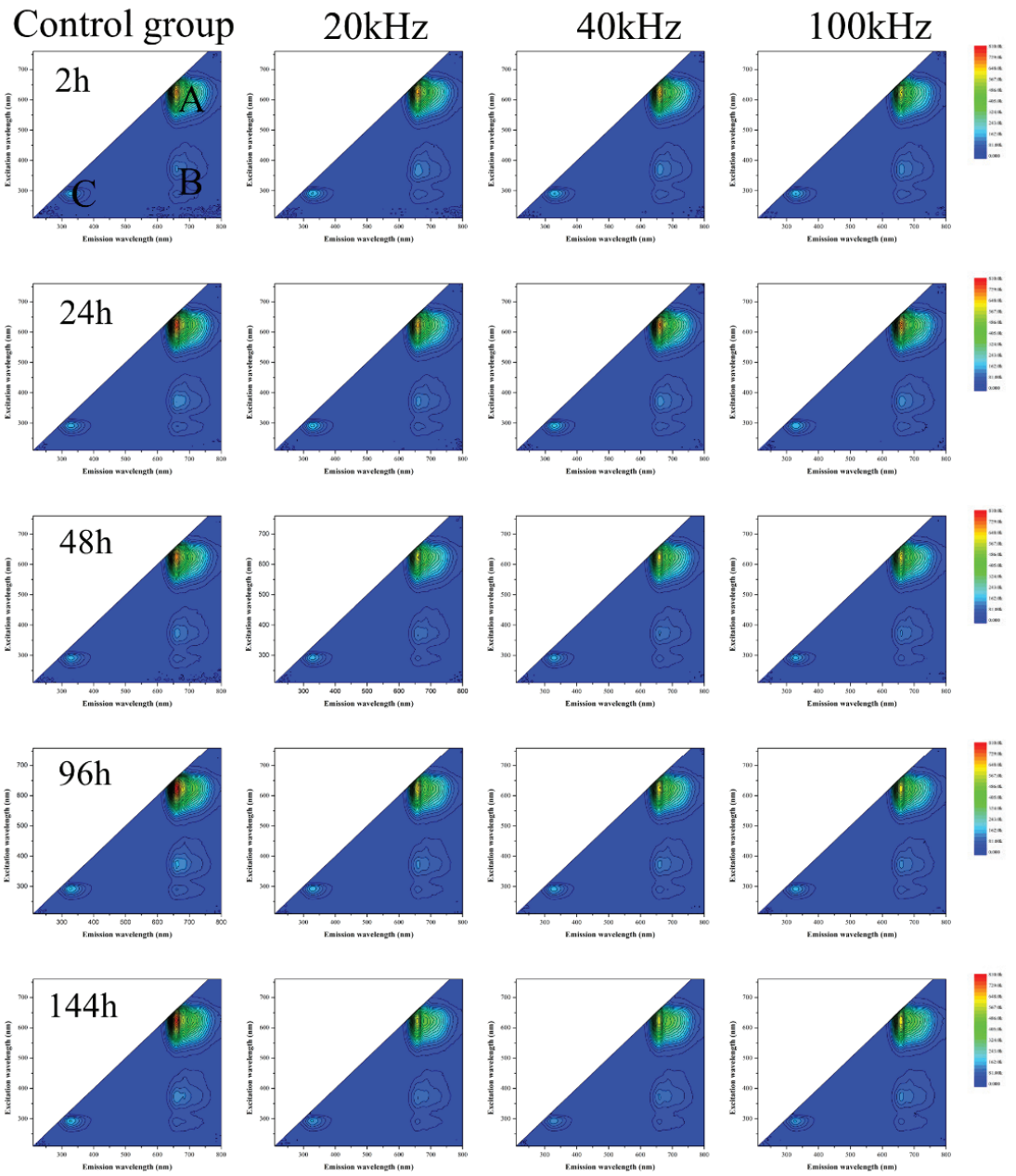

Fig. 2. The three-dimensional EEM fluorescence spectra after ultrasonic irradiation with different frequencies and a fixed power density of 0.013 W/mL.

within 2–144 h. This result explained that the algal cells grew well. In 2 h, the fluorescence peak of Peak B increased gradually. *M. aeruginosa* fragment can absorb ammonia nitrogen (reach equability in 30 min), and the adsorption process was in conformity with the Henry adsorption isotherm [36]. Thus, the change in the trend of Peak B was probably due to the absorption of the protein substance by the death of algal cells [37]. The fluorescence peak of peaks A and C increased gradually due to ultrasonic treatment. Subsequently, the algal cells of the experimental groups began to recover, and the fluorescence peaks of A, B, and C increased. The increase might be because cellular repair mechanism was unable to return to the initial level of the fluorescence peak after the ultrasonic treatment. The increase showed that ultrasound exhibited definite inhibitory effect on the growth of algal cells. The greater the power density is, the lower the recovery level of algal cells would be.

3.2.3. Effect of ultrasonic irradiation on IOM three-dimensional EEM of algae cells

Three-dimensional EEM fluorescence spectra of IOM under ultrasound with different frequencies and a fixed power density of 0.013 W/mL are presented in

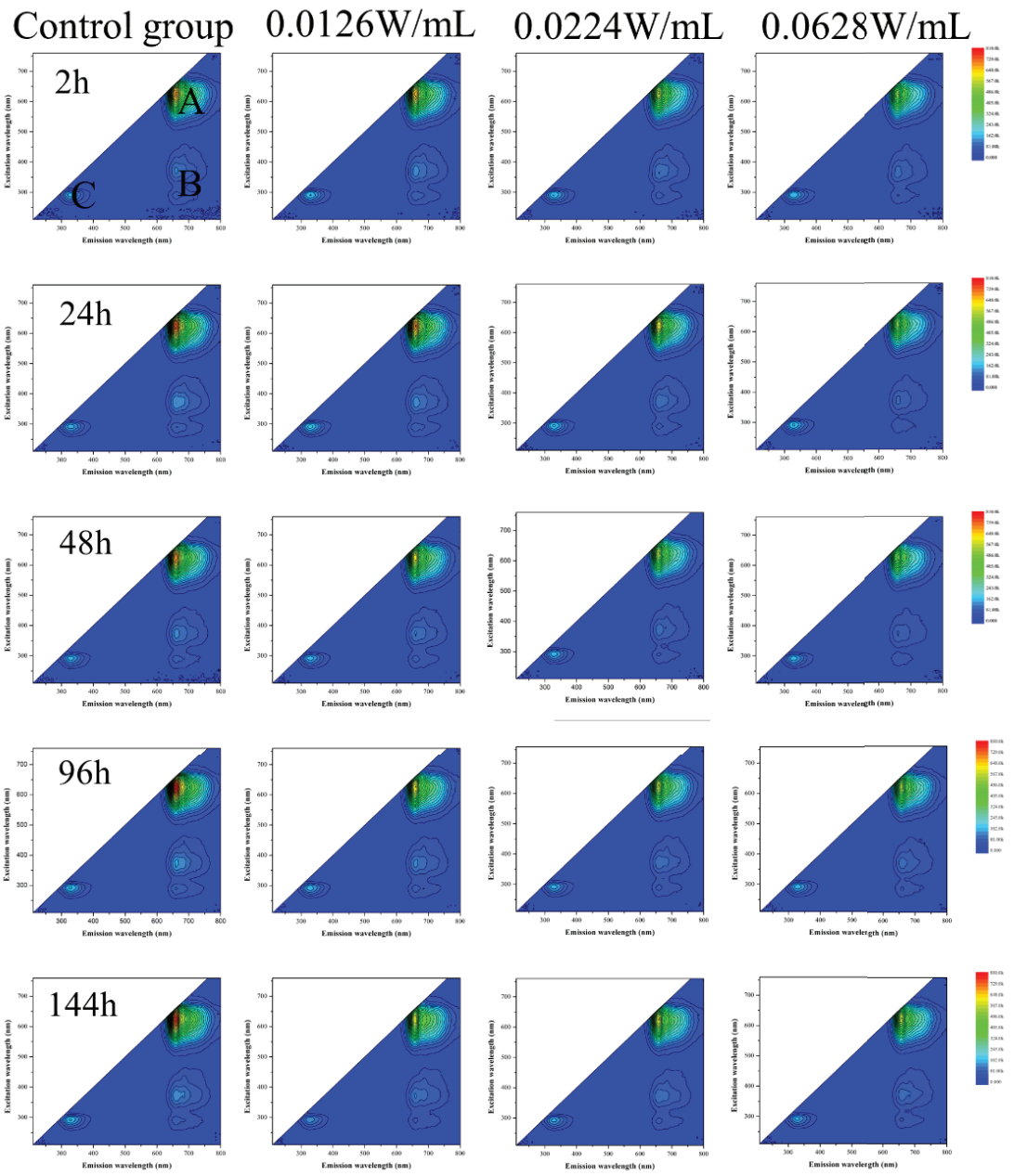

Fig. 3. The three-dimensional EEM fluorescence spectra after ultrasonic irradiation with different power densities and a fixed frequency of 40 kHz.

Fig. S4. The three kinds of fluorescence peaks included in the spectra are peaks A and B (soluble metabolites) E_x/E_m = (270–290) nm/(300–350) nm and E_x/E_m = (220–230) nm/(330–350) nm, Peak C (fulvic acid in the ultraviolet region), E_x/E_m = (260–275) nm/(421–464) nm [34,35]. As seen in Fig. S4, peaks A and B of the algal cells continued to rise in the control group within 2–144 h. The peaks A and B were higher than the three-dimensional EEM fluorescence spectra of EOM, which represented soluble metabolites. In the first two hours, the fluorescence peaks of A and B in the experimental groups decreased slightly. The results demonstrated that intact algal cells had ruptured partially under ultrasound, and the intracellular substances were released into the solution. In 24–144 h, the fluorescence peak of algal cells began to rise but that was lower than the control group.

Three-dimensional EEM fluorescence spectra of IOM under ultrasound with different power densities and a fixed frequency of 40 kHz are presented in Fig. S5. The peaks A and B of the algal cells continued to rise in the control group within 2–144 h. This result explained that the algal cells grew well. In 2 h, the fluorescence peaks of A and B decreased with the increase in the ultrasonic power density corresponding to the increased fluorescence peak of soluble metabolites in EOM. In 2 h, the fluorescence peaks of A and B decreased

through increased power density, which represents the increase fluorescence peak of soluble metabolites in three-dimensional EEM fluorescence spectra of EOM. The results showed that the cells rupture of algae in the solution and the release of intracellular substance increase as the ultrasonic power density increases. The increase of power density resulted in the increase of the fluorescence peaks of C and D. The results demonstrated that the death of the cells increased. Subsequently, the algal cells began to recover but were unable to return to the initial level (see Section 3.2.2).

3.3. The photosynthetic protein

RuBisCO protein is a key enzyme in the dark reaction to fix the CO_2 [38]. RuBisCO protein exhibited catalytic activity of carboxylase and oxygenase and can associate carbon assimilation with photorespiration.

The changes in the RuBisCO protein under ultrasound exposure with different ultrasonic frequencies and a fixed power density of 0.013 W/mL are shown in Fig. 4(a). In 72 h, different ultrasonic frequencies (20, 40, and 100 kHz) made unfavorable effect on the RuBisCO protein. The relative content of RuBisCO protein in each experimental group decreased to 77.4%, 69.0%, and 76.8%. The degree of damage under ultrasonic frequency of 40 kHz was larger than that of 20 and 100 kHz, and the difference of RuBisCO protein damage was insignificant between the ultrasonic frequency of 20 kHz and the ultrasonic frequency of 100 kHz (Fig. 4(b)). The rbcL gene is the coding gene of RuBisCO protein.

The changes in the RuBisCO protein under ultrasound exposure with different ultrasonic power densities and a fixed frequency of 40 kHz are shown in Fig. 4(c). Combined with Fig. 4(d), the greater the power density was, the lower was the grey density of RuBisCO protein bands. The results showed that the greater the ultrasonic power density, the greater the effect on the photosynthesis of algal cells.

3.4. Phycobiliprotein of algae

The phycobiliprotein in *M. aeruginosa* can be divided into three types: PC, PE, and APC. Photosynthesis is transmitted to the reaction center by phycoerythrocyin, PC, and chlorophyll a after being captured by phycobilisomes.

The changes in phycobiliprotein under ultrasound exposure at different ultrasonic frequencies and a fixed power density of 0.013 W/mL are shown in Fig. 5. The relative content of phycobiliprotein reached the lowest value at 2 h, which was about 40%. The results showed that the degree of the immediate damage to algae at different frequencies (20, 40, and 100 kHz) were similar with fixed power density. The results also showed that as the culture time increased, the change trend of phycobiliprotein was first increased and then decreased. The relative content of phycobiliprotein in algal cells was greater than that of control group at 96 h with the frequency of 100 kHz, and this phenomenon might be because the algal cells exhibited a stress response to external disturbances. After 96 h, the relative content of phycobiliprotein increased negligibly or even decreased. From Fig. 5(b), the change trend of PC was similar to the Peak A in Fig. 2. The algal cells did start the repair mechanism. By the experimental results, 40 kHz group reduced the relative content of phycobiliprotein significantly.

The changes in phycobiliprotein under different ultrasonic power densities and a fixed ultrasonic frequency of 40 kHz are shown in Fig. 6. The total trend of the relative content of phycobiliprotein first decreased rapidly, then

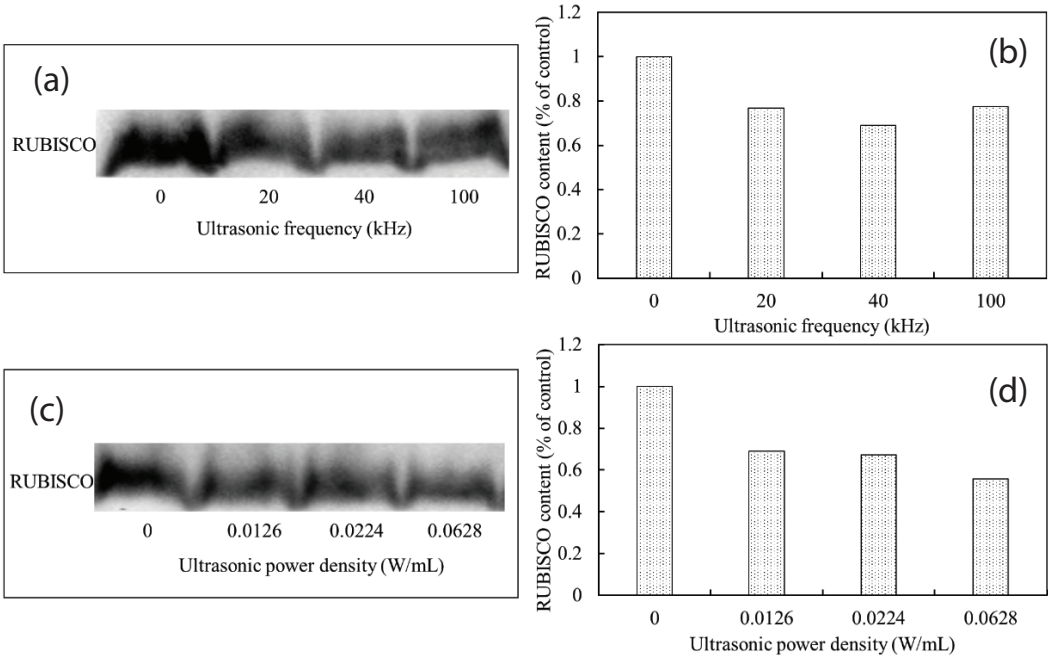

Fig. 4. Change in the RuBisCO protein after ultrasonic irradiation for 72 h of (a) gel electrophoresis and (b) content of RuBisCO with different frequencies and a fixed power density of 0.013 W/mL, and (c) gel electrophoresis and (d) content of RuBisCO with different power densities and a fixed frequency of 40 kHz.

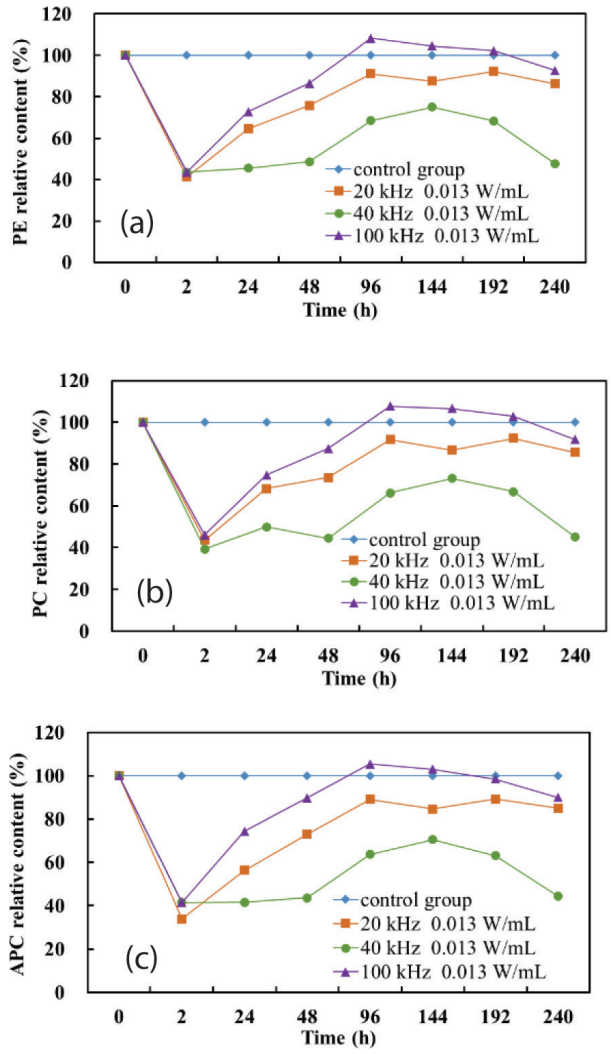

Fig. 5. Change in phycobiliprotein after ultrasonic irradiation with different frequencies and a fixed power density of 0.013 W/mL: (a) PE, (b) PC, and (c) APC.

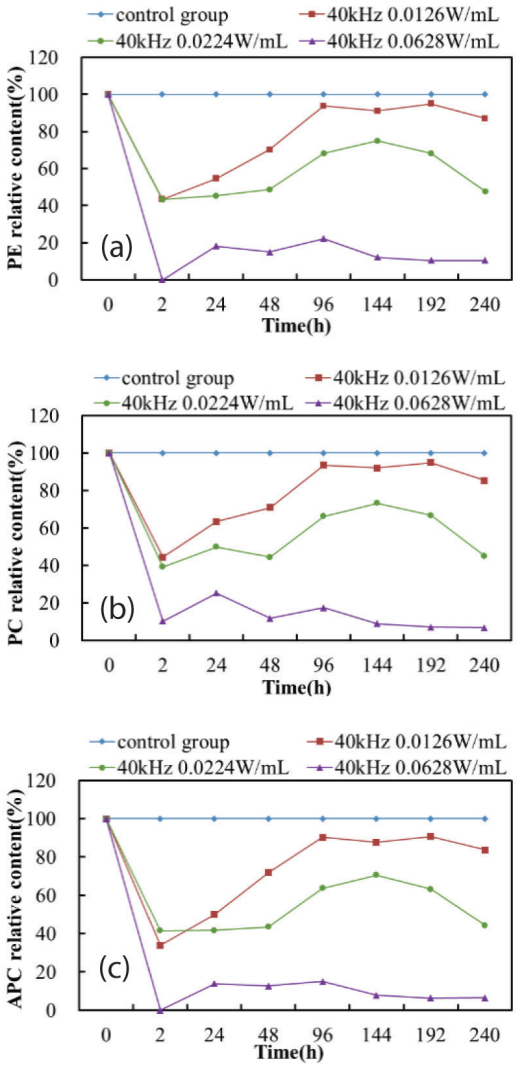

Fig. 6. Change in phycobiliprotein after ultrasonic irradiation with different power densities and a fixed frequency of 40 kHz: (a) PE, (b) PC, and (c) APC.

increased, and finally decreased slowly. From Fig. 6(a), the relative content of PE had plunged to 0 with the frequency of 40 kHz and power density of 0.0628 W/mL which signed that PE had been destroyed completely. The relative content of PE was approximately 43% with the frequency of 40 kHz and power densities of 0.0126 and 0.0224 W/mL. The relative content of phycobiliprotein started to rise after 2 h; the greater the power density was, the higher was the level of the recovery of PE. The content of PE in the experimental group with the frequency of 40 kHz and the power density of 0.0126 W/mL recovered to the initial level when cultured to 96 h (relative component as 94%), and the content showed unobvious change. The trend of PC and APC was similar to that of PE.

According to experimental results, the trend of different experimental groups was similar. Although some algal cells could be repaired, it could not be repaired completely due to ultrasound. These findings suggest that ultrasound destroyed the light energy transfer chain by destroying phycobiliprotein.

3.5. The effect of ultrasonic frequency on the algal density

Generally, blood cell counting method and OD_{560} measured by fluorescence spectrophotometer are the common methods to determine the number of algal cells. The first method spends a lot of time. Therefore, the second method was used in this study because it is simple and rapid. Variation of the inhibition rate of algal cells after ultrasonic irradiation with different ultrasonic frequencies and a fixed power density of 0.013 W/mL is shown in Figs. 7(a) and (b). In 2 h, the effect of ultrasound on the growth inhibition of algal cells was most obvious, the inhibition rate of experimental groups were 1547%, 1069%, and 1256%. The algal density increased continuously with the increase of culture time. The algal density in different experimental groups was close to 96 h, but the algal density of the experimental group was lower than that of the control group (Fig. 7(a)). This showed that the growth of the algal cells after 96 h was inhibited after ultrasonic treatment. The inhibition rate was greater than 0, which indicated that ultrasound played a

certain role in inhibiting the growth of algal cells. However, the experimental results showed that the effect of different frequencies with a fixed power density on algal cells density was not obvious; the algal density in the experimental group began to increase in the late stage, which was similar to the experimental results of Rajasekhar et al. [39].

3.6. Interaction mechanisms

The results showed that the mechanism of ultrasound on algal cells mainly included mechanical action and cavitation effect [40]. Fig. 8 showed a rapid decrease in fluorescence peak when the samples were treated by ultrasound in 40 kHz and 0.0628 W/mL for 2 h, which presented the degradation of B peak's intensity and the increase of A and C peaks' intensity of EOM and EEM, whereas the variation trend of IOM was just opposite. We previously investigated whether ultrasonic irradiation in water produced free radicals. The results showed that ca 0.5 μmol/L hydroxyl radical (·OH) was produced under the frequency of 40 kHz [41]. Hence, acute cell damage caused by acute erosion and oxidation of algal cells after ultrasonic treatments may be attributed to the generation of ·OH during

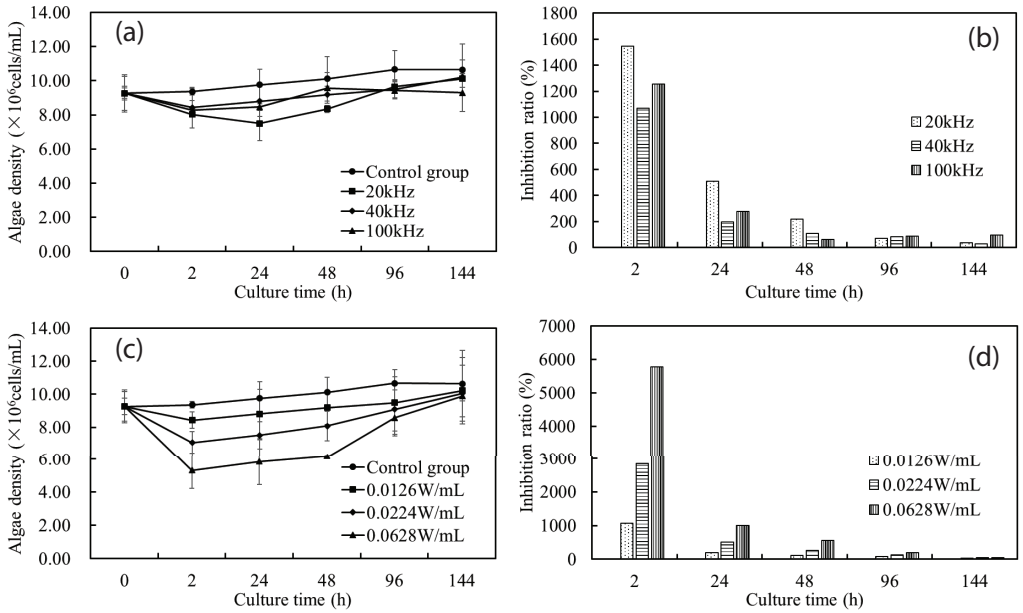

Fig. 7. Change in algal density (a) and inhibitory rate (b) after ultrasonic irradiation with different frequencies and a fixed power density of 0.013 W/mL, and change in algal density (c) and inhibitory rate (d) after ultrasonic irradiation with different power densities and a fixed frequency of 40 kHz.

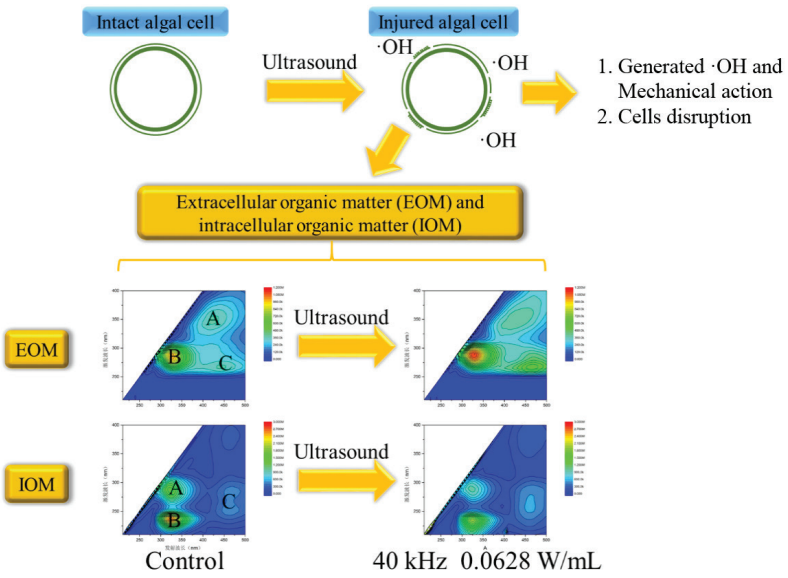

Fig. 8. Interaction mechanism of ultrasound on algae.

cavitation effect and its strong oxidizability [42]. The changes in EOM and IOM were mainly based on the changes in the cells themselves, as reflected by the slow increase in the EOM class humus peak and slow reduction of IOM. Meanwhile, the algal cell inhibition rate reached the maximum at 2 h after the inhibition rate decreased at 2–144 h in the experimental groups, which indicates that the process may be relative to the cellular repair mechanisms. The metabolism of experimental group was slower, which showed that ultrasonic treatments played a certain role in inhibiting the growth of algae cells.

4. Conclusion

After certain ultrasonic treatments, algae cells were self-healing, but the algae density of the experimental groups and the absolute value of zeta potential were always lower than those of the control groups. EEM spectrum showed that the fluorescence peak value of the fluvic acid-like substances in treated samples increased, which may be attributed to increased cell deaths. The phycobiliprotein content of the treated samples dropped dramatically after ultrasonic treatments. These results suggest that the ultrasonic frequency and power density in the range of 40 kHz and 0.0628 W/mL may be useful in controlling growth and reproduction of algae, respectively.

Acknowledgments

The authors gratefully acknowledge the financial support from the National Natural Science Foundation of China (Nos. 51308123 and 51778146), the Outstanding Youth Fund of Fujian Province in China (No. 2018J06013), the China Postdoctoral Science Foundation (No. 2014M561856), and the open test fund for valuable instruments and equipment of Fuzhou University (No. 2018T033).

References

[1] T. Krüger, C. Wiegand, K. Li, B. Luckas, S. Pflugmacher, More and more toxins around–analysis of cyanobacterial strains isolated from Lake Chao (Anhui Province, China), Toxicon, 56 (2010) 1520–1524.
[2] L. Peng, Y. Liu, W. Chen, L. Liu, M. Kent, L. Song, Health risks associated with consumption of microcystin-contaminated fish and shellfish in three Chinese lakes: significance for freshwater aquacultures, Ecotoxicol. Environ. Saf., 73 (2010) 1804–1811.
[3] L. Pearson, T. Mihali, M. Moffitt, R. Kellmann, B. Neilan, On the chemistry, toxicology and genetics of the cyanobacterial toxins, microcystin, nodularin, saxitoxin and cylindrospermopsin, Mar. Drugs, 8 (2010) 1650–1680.
[4] T.G. Otten, H. Xu, B. Qin, G. Zhu, H.W. Paerl, Spatiotemporal patterns and ecophysiology of toxigenic microcystis blooms in Lake Taihu, China: implications for water quality management, Environ. Sci. Technol., 46 (2012) 3480–3488.
[5] H.W. Paerl, V.J. Paul, Climate change: links to global expansion of harmful cyanobacteria, Water Res., 46 (2012) 1349–1363.
[6] Y. Tao, X. Mao, J. Hu, H.O.L. Mok, L. Wang, D.W.T. Au, J. Zhu, X. Zhang, Mechanisms of photosynthetic inactivation on growth suppression of *Microcystis aeruginosa* under UV-C stress, Chemosphere, 93 (2013) 637–644.
[7] P. Rajasekhar, L. Fan, T. Nguyen, F.A. Roddick, A review of the use of sonication to control cyanobacterial blooms, Water Res, 46 (2012) 4319–4329.
[8] C. Svrcek, D.W. Smith, Cyanobacteria toxins and the current state of knowledge on water treatment options: a review, J. Environ. Eng. Sci., 3 (2004) 155–185.
[9] T.J. Lee, K. Nakano, M. Matsumare, Ultrasonic irradiation for blue-green algae bloom control, Environ. Technol., 22 (2001) 383–390.
[10] G. Zhang, P. Zhang, B. Wang, H. Liu, Ultrasonic frequency effects on the removal of *Microcystis aeruginosa*, Ultrason. Sonochem., 13 (2006) 446–450.
[11] D. Purcell, S.A. Parsons, B. Jefferson, The influence of ultrasound frequency and power, on the algal species *Microcystis aeruginosa*, *Aphanizomenon flos-aquae*, *Scenedesmus subspicatus* and *Melosira* sp., Environ. Technol., 34 (2013) 2477–2490.
[12] A.K. Klemenčic, T.G. Bulc, D. Balabanic, The effectiveness of chemical-free water treatment system combining fibre filters, ultrasound, and UV for fish farming on algal control., Period. Biol., 112 (2010) 211–217.
[13] G. Fan, Z. Zhang, J. Luo, X. Wan, C. Liu, Response surface design for the optimization of *Chlorella pyrenoidosa* removal by low frequency ultrasonic irradiation, Asian J. Chem., 25 (2013) 202–208.
[14] G. Fan, D. Liu, G. Zhu, Q. Lin, L. Chen, Influence factors in kinetics during removal of harmful algae by ultrasonic irradiation process, Desal. Wat. Treat., 52 (2014) 7317–7322.
[15] R.K. Henderson, A. Baker, S.A. Parsons, B. Jefferson, Characterisation of algogenic organic matter extracted from cyanobacteria, green algae and diatoms, Water Res., 42 (2008) 3435–3445.
[16] T. Li, B.Z. Dong, Z. Liu, Characteristic of algogenic organic matter (AOM) and its effect on UF membrane fouling, Huanjing Kexue, 31 (2010) 318–323.
[17] C. Liu, J. Wang, Z. Cao, W. Chen, H. Bi, Variation of dissolved organic nitrogen concentration during the ultrasonic pretreatment to *Microcystis aeruginosa*, Ultrason. Sonochem., 29 (2016) 236–243.
[18] D. Purcell, Control of Algal Growth in Reservoirs with Ultrasound, Cranfield University, UK, 2009.
[19] G. Fan, W. Chen, J. Luo, R. Xu, X. Lin, X. Zheng, H. Peng, Damaging effects of ultrasonic treatment on the photosynthetic system of *Microcystis aeruginosa*, Desal. Wat. Treat., 78 (2017) 350–359.
[20] S. Zhou, Y. Shao, N. Gao, D. Yang, L. Lei, D. Jing, C. Tan, Characterization of algal organic matters of *Microcystis aeruginosa*: biodegradability, DBP formation and membrane fouling potential, Water Res., 52 (2014) 199–207.
[21] Y. Tang, J. Tian, S. Li, C. Xue, Z. Xue, D. Yin, S. Yu, Combined effects of graphene oxide and Cd on the photosynthetic capacity and survival of *Microcystis aeruginosa*, Sci. Total Environ., 532 (2015) 154–161.
[22] F. Qu, H. Liang, Z. Wang, H. Wang, H. Yu, G. Li, Ultrafiltration membrane fouling by extracellular organic matters (EOM) of *Microcystis aeruginosa* in stationary phase: influences of interfacial characteristics of foulants and fouling mechanisms, Water Res., 46 (2012) 1490–1500.
[23] C. Tian, T.T. Guo, R.P. Liu, W. Jefferson, H.J. Liu, Q.U. Jiu-Hui, Formation of disinfection by-products by *Microcystis aeruginosa* intracellular organic matter: comparison between chlorination and bromination, Environ. Sci., 34 (2013) 4282–4289.
[24] C. Six, L. Joubin, F. Partensky, J. Holtzendorff, L. Garczarek, UV-induced phycobilisome dismantling in the marine picocyanobacterium *Synechococcus* sp. WH8102., Photosynth. Res., 92 (2007) 75–86.
[25] OECD, Sixteenth Addendum to the OECD Guidelines for the Testing of Chemicals, OECD, Paris, France, 2006.
[26] G.J. Jameson, Hydrophobicity and floc density in induced-air flotation for water treatment 1, Colloids Surf. A, 151 (1999) 269–281.
[27] L. Parent, M.R. Twiss, P.G.C. Campbell, Influences of natural dissolved organic matter on the interaction of aluminum with the microalga *Chlorella*: a test of the free-ion model of trace metal toxicity, Environ. Sci. Technol., 30 (1996) 1713–1720.
[28] M. Pivokonsky, O. Kloucek, L. Pivokonska, Evaluation of the production, composition and aluminum and iron complexation of algogenic organic matter., Water Res., 40 (2006) 3045–3052.
[29] A. Baker, Fluorescence excitation–emission matrix characterization of some sewage-impacted rivers, Environ. Sci. Technol., 35 (2001) 948–953.

[30] J. Seppälä, M. Balode, The use of spectral fluorescence methods to detect changes in the phytoplankton community, Hydrobiologia, 363 (1997) 207–217.
[31] J.A. Korak, E.C. Wert, F.L. Rosario-Ortiz, Evaluating fluorescence spectroscopy as a tool to characterize cyanobacteria intracellular organic matter upon simulated release and oxidation in natural water, Water Res., 68 (2015) 432–443.
[32] W. Chen, P. Westerhoff, J.A. Leenheer, K. Booksh, Fluorescence excitation–emission matrix regional integration to quantify spectra for dissolved organic matter., Environ. Sci. Technol., 37 (2003) 5701–5710.
[33] Y. Tao, X. Zhang, D.W. Au, X. Mao, K. Yuan, The effects of sub-lethal UV-C irradiation on growth and cell integrity of cyanobacteria and green algae, Chemosphere, 78 (2010) 541–547.
[34] C. Liu, J. Wang, W. Chen, H. Zhu, H. Bi, Characterization of DON in IOM derived from *M. aeruginosa* and its removal by sunlight/immobilized TiO_2 system, RSC Adv., 5 (2015) 41203–41209.
[35] T. Guo, Y. Yang, R. Liu, X. Li, Enhanced removal of intracellular organic matters (IOM) from *Microcystic aeruginosa* by aluminum coagulation, Sep. Purif. Technol., 189 (2017) 279–287.
[36] H. Shing, H. Liu, J. Qu, R. Dai, The property of adsorption about ammonium on debris of *Microcystis* cells in eutrophic water, Environ. Chem., 24 (2005) 241–244.
[37] Y. Zhang, W. Liang, Y. Zhao, F. Li, J. Cao, S. Hu, Generation and release of Microcystin-IR by *Microcystis aeruginosa* under hydroquinone inhibition, Environ. Sci., 35 (2014) 2294–2299.
[38] T.M. Macdonald, L. Dubois, L.C. Smith, D.A. Campbell, Sensitivity of cyanobacterial antenna, reaction center and CO_2 assimilation transcripts and proteins to moderate UVB: light acclimation potentiates resistance to UVB., Photochem. Photobiol., 77 (2003) 405–412.
[39] P. Rajasekhar, L. Fan, T. Nguyen, F.A. Roddick, Impact of sonication at 20kHz on *Microcystis aeruginosa*, *Anabaena circinalis* and *Chlorella* sp., Water Res., 46 (2012) 1473–1481.
[40] M. Kurokawa, P.M. King, X. Wu, E.M. Joyce, T.J. Mason, K. Yamamoto, Effect of sonication frequency on the disruption of algae, Ultrason. Sonochem., 31 (2016) 157–162.
[41] G. Fan, W. Chen, Z. Su, R. Lin, R. Xu, X. Lin, Q. Zhong, Preventive inhibition mechanism of algae by ultrasound based on analysis of physiological characteristics, Desal. Wat. Treat., 68 (2017) 70–79.
[42] H. Miao, W. Tao, The mechanisms of ozonation on cyanobacteria and its toxins removal, Sep. Purif. Technol., 66 (2009) 187–193.

Supporting information

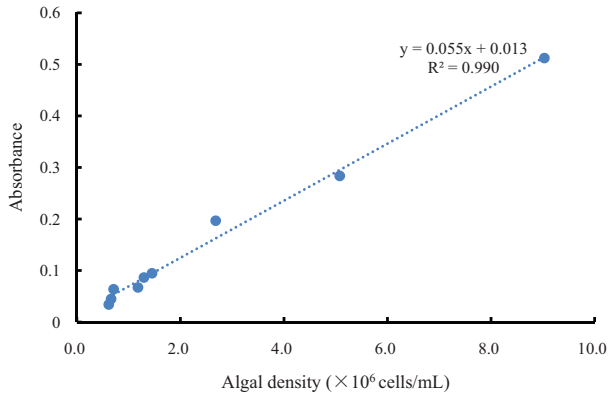

Fig. S1. The standard curves of algae density and absorbance.

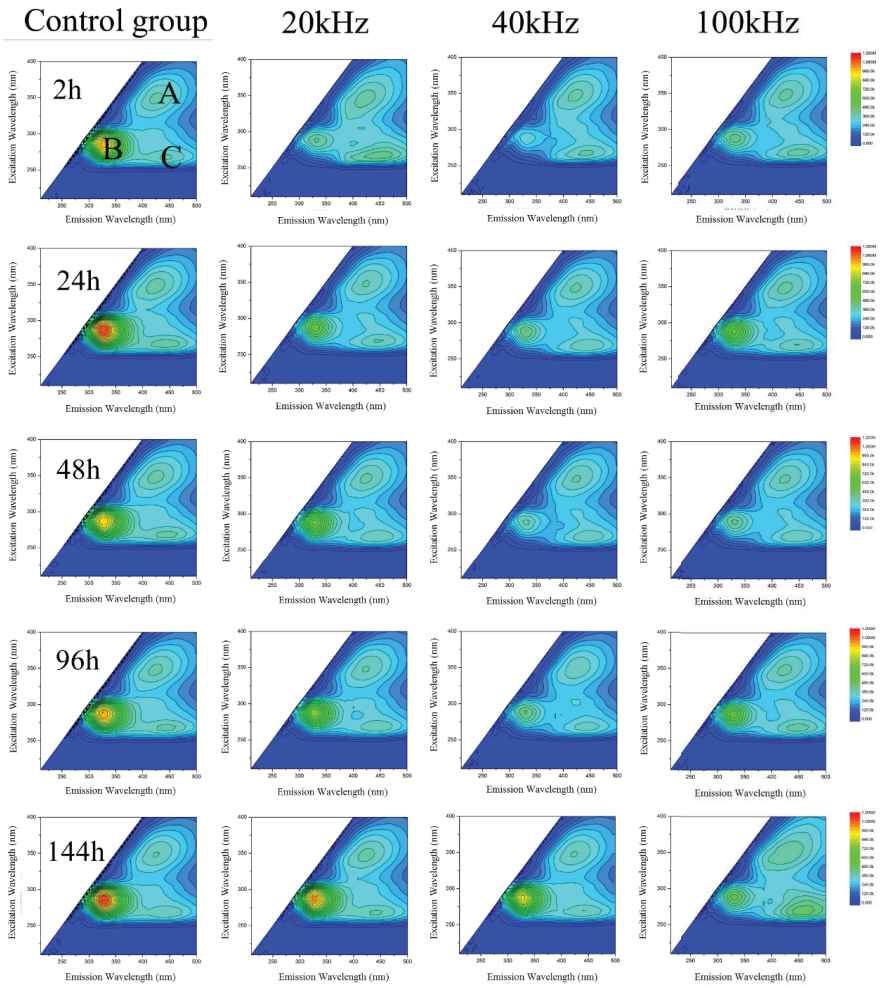

Fig. S2. The three-dimensional EEM fluorescence spectra of EOM after ultrasonic irradiation with different frequencies and a fixed power density of 0.013 W/mL.

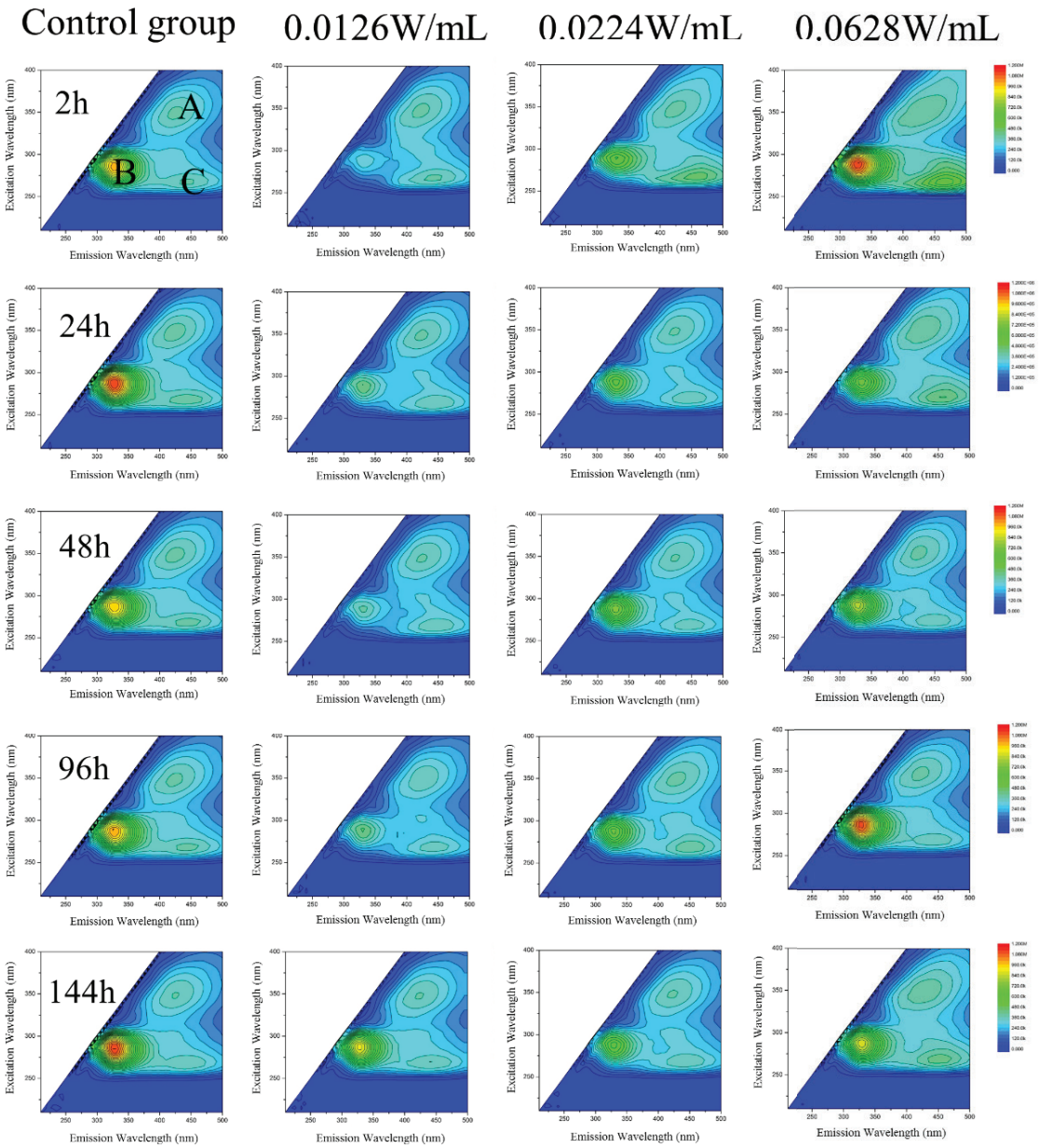

Fig. S3. The three-dimensional EEM fluorescence spectra of EOM after ultrasonic irradiation with different power densities and a fixed frequency of 40 kHz.

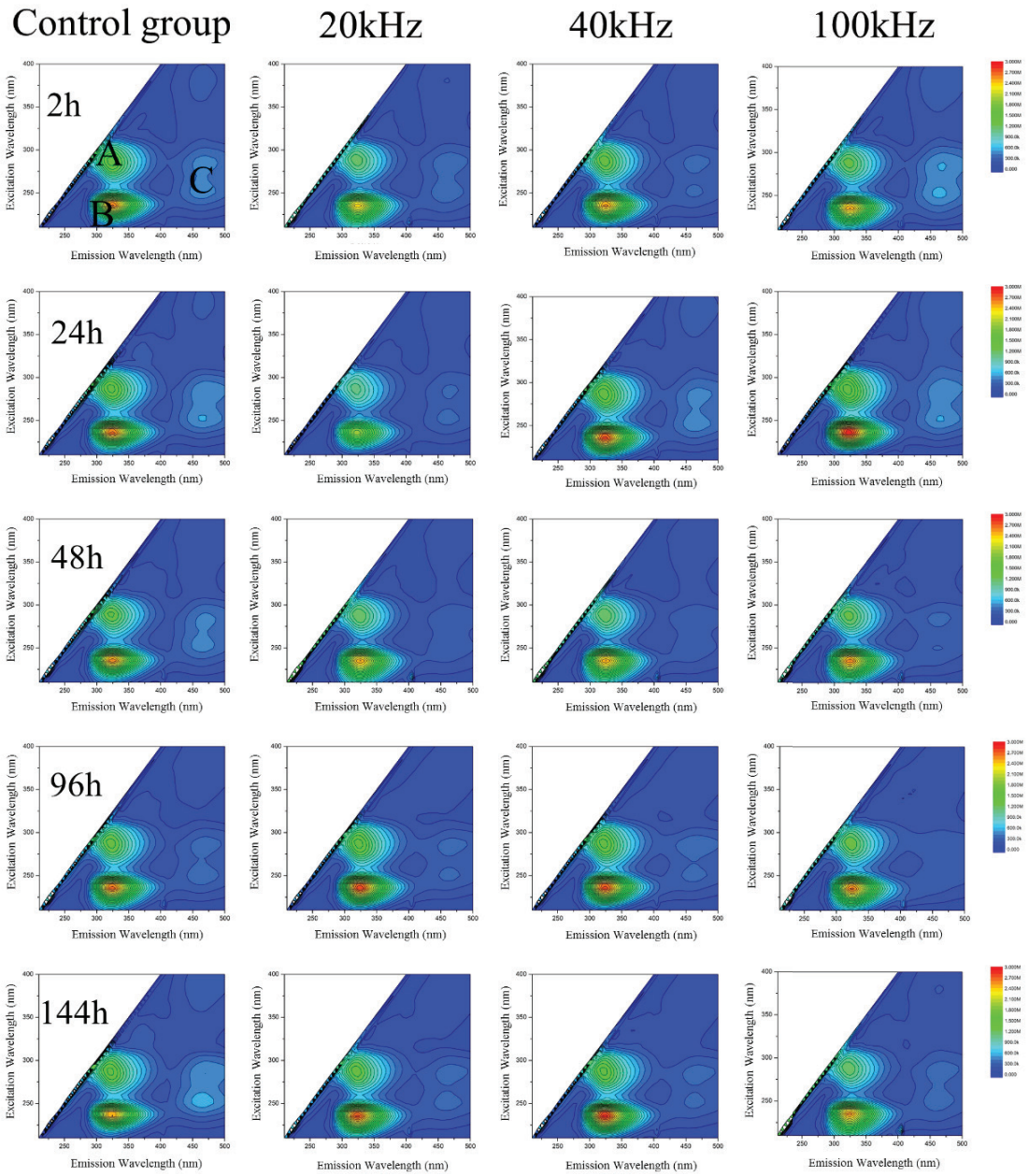

Fig. S4. The three-dimensional EEM fluorescence spectra of IOM after ultrasonic irradiation with different frequencies and a fixed power density of 0.013 W/mL.

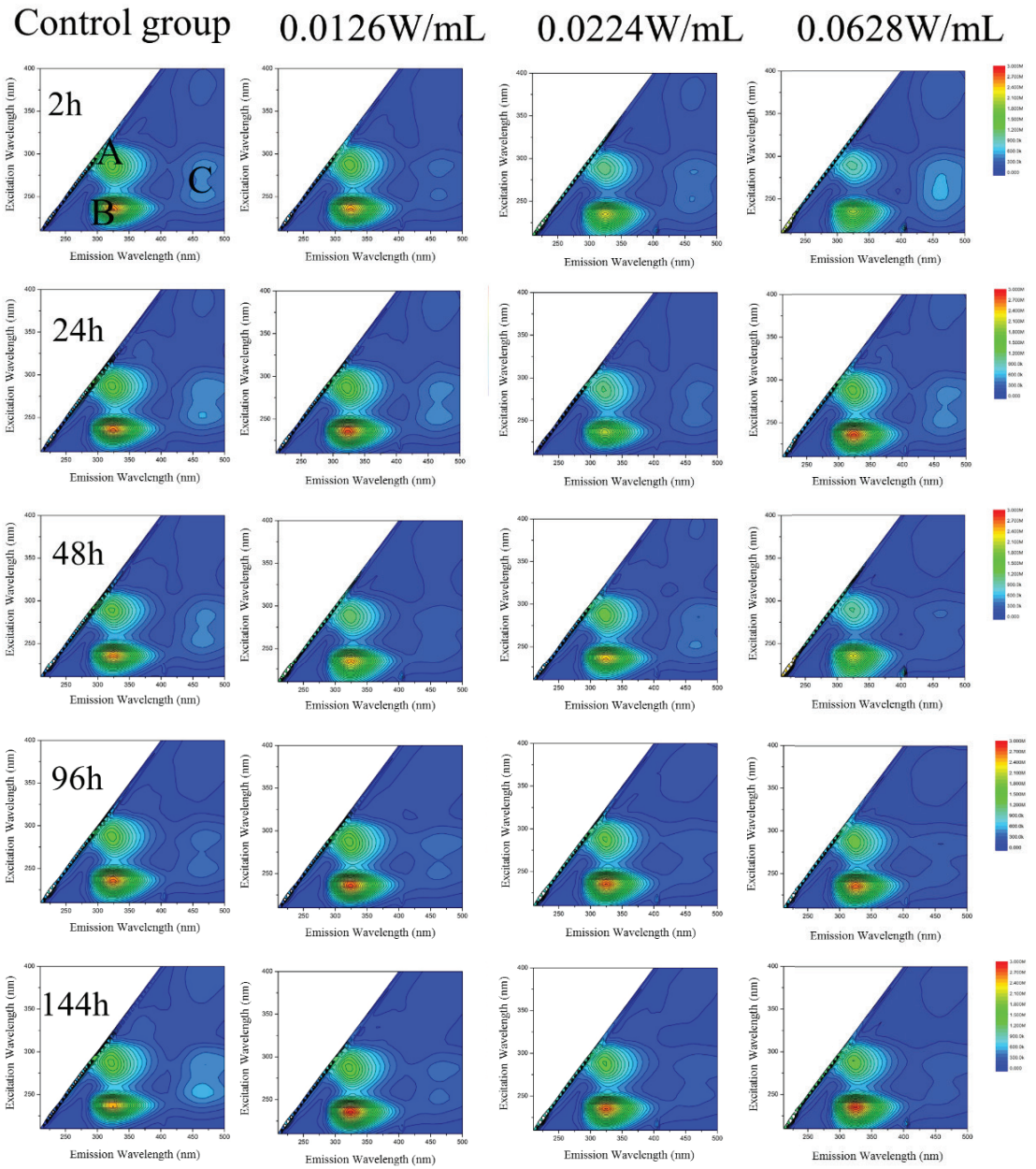

Fig. S5. The three-dimensional EEM fluorescence spectra of IOM after ultrasonic irradiation with different power densities and a fixed frequency of 40 kHz.